

Molecular Orientation Effects on Hydrogen Transfer Rates Under Diffusional Constraints

Michelle K. Kidder, A.C. Buchanan, III, and Phillip F. Britt

Chemical Sciences Division
Oak Ridge National Laboratory
Bethel Valley Road
P.O. Box 2008, MS-6197
Oak Ridge, Tennessee 37831-6197

Research sponsored by the Division of Chemical Sciences, Geosciences, and Biosciences, Office of Basic Energy Sciences, U.S. Department of Energy, under contract DE-AC05-00OR22725 with Oak Ridge National Laboratory, managed and operated by UT-Battelle, LLC.

"The submitted manuscript has been authored by a contractor of the U.S. Government under contract No. DE-AC05-00OR22725. Accordingly, the U.S. Government retains a nonexclusive, royalty-free license to publish or reproduce the published form of this contribution, or allow others to do so, for U.S. Government purposes."

Introduction

The kinetics, conversion efficiency and product quality during thermal processing of fossil and renewable energy resources into fuels or chemicals is impacted by restricted diffusion imposed by the cross-linked, macromolecular network structure. There has been limited understanding of how these macroscopic effects are rooted in alterations in the underlying reaction pathways (radical, ionic, catalytic, etc.). We have developed model systems that address restricted diffusion effects by immobilizing fuel model compounds onto silica surfaces.¹⁻² The Si-O-C_{aryl} linkage that forms from the condensation of the phenolic precursor with the surface silanols of a high purity, nonporous, fumed silica is thermally robust, up to ca. 550°C, but is readily hydrolyzed in aqueous base such that surface-attached products can be recovered for analysis.¹

Previous studies of surface-immobilized systems found that thermal decomposition reaction rates and product selectivities can be significantly different than that of analogous liquid and vapor phase reactions. Our recent research has focused on two component systems to explore the effects of hydrogen donor and non-hydrogen donor spacers. In the decomposition of surface-immobilized 1, 3-diphenylpropane (DPP), we found that hydrogen donor spacer molecules could accelerate the pyrolysis rate up to ca. 80 fold compared to that of non-donor spacers.¹ This phenomenon is unique to the surface and attributable to the diffusional constraints, since the pyrolysis rate of DPP in solution does not depend on the structure of the diluent. Experiments with a deuterium labeled spacer provided additional evidence for a process involving a series of rapid hydrogen transfer steps with free radical intermediates on the surface. This process provides a mechanism for radical centers to rapidly relocate in a diffusionally constrained environment without the need for physical movement. We have now expanded this research to investigate the possible impact of molecular orientation by examining isomeric spacers with hydrogen donor capabilities, and their influence on the rate and selectivities of thermal decomposition of surface-immobilized DPP. The surfaced-immobilized spacer molecules being investigated include 2-hydroxyfluorene, 3-hydroxyfluorene, 1-hydroxytetralin, 2-hydroxytetralin, 2-hydroxy-9, 10-dihydrophenanthrene and 3-hydroxy-9, 10-dihydrophenanthrene.

Experimental

GC analysis was performed on a Hewlett Packard 5890 Series II gas chromatograph employing a J & W Scientific 30 m x 0.25 mm DB-1 methylsilicone column (0.25 μm film thickness) and flame ionization detection. Detector response factors were determined relative to cumene (hydrocarbon products) or 2, 5-dimethylphenol and *p*-hydroxy biphenyl, *p*-HOBP, (phenolic products) as internal standards. Mass spectra were obtained at 70 eV with a Hewlett Packard 5972A/5890 Series II GC-MS equipped with a capillary column matched to that used for GC analyses.

Materials. Cabosil M-5, (200 m²/g, ca. 4.5 SiOH/nm² or 1.5 mmol SiOH/g) was purchased from Cabot Corp., dried at 200 °C for 4 hours, and cooled in a desiccator before use. Benzene was distilled from sodium. High purity acetone and dichloromethane were commercially available and used as received. Cumene was fractionally distilled (2x) and 2,5-dimethylphenol was

recrystallized from ethanol. *p*-Hydroxy biphenyl, 5,6,7,8- tetrahydro-2-naphthol (2-hydroxytetralin, or 2-HOTET) and 5,6,7,8-tetrahydro-1-naphthol (or 1-hydroxy tetralin, 1-HOTET) were commercially available and purified by repeated recrystallizations from benzene/hexane. The synthesis of *p*-(3-phenylpropyl)phenol (HODPP) and 2-hydroxyfluorene (2-HOFI) were previously described^{1a, 3a}. The multi-step synthesis of the 3-hydroxyfluorene (3-HOFI), 2-hydroxy-9, 10-dihydrophenenanthrene (2-HODHP), and 3-hydroxy-9, 10-dihydrophenanthrene (3-HODHP) precursors will be reported elsewhere.

Preparation of Surface-Attached Materials. Procedures for the preparation of the two component surfaces have been described previously¹. In general, HODPP and the desired spacer phenol were dissolved in benzene in the appropriate mol ratios, and then were added to a benzene slurry containing Cabosil. The benzene was evaporated and the phenolic material was attached to the surface through heating at 225 °C for 1 h in an evacuated (2×10^{-6} torr) sealed Pyrex tube. Unattached phenols were removed via sublimation at 225-275 °C for 1 h under dynamic vacuum (5×10^{-3} torr). Surface coverage analysis was performed as described previously² using *p*-HOBP as the internal standard.

Pyrolysis Procedure. The pyrolysis apparatus and procedure have been described previously.^{1,2} In brief, a weighed amount of sample was placed in a T-shaped Pyrex tube, evacuated and sealed at ca. 2×10^{-6} torr. The sample was pyrolyzed in a pre-heated calibrated Carbolite tube furnace, and the arm of the tube was placed in liquid nitrogen to trap the gas phase products. The volatile products collected in the trap were dissolved in acetone (50-150 μ L) containing the internal standards, and the solution was analyzed via GC and GC-MS. Surface-attached pyrolysis products were hydrolyzed from the silica with 1N NaOH. The internal standards, 2, 5-dimethylphenol and HOBP were prepared in NaOH and added to the solution. The solution was acidified and extracted with CH_2Cl_2 , evaporated, then silylated with a mixture of *N, O*-bis(trimethylsilyl)-trifluoroacetamide (BSTFA)/pyridine 1:2 (ca. 300 μ L) and analyzed via GC and GC-MS.

Results and Discussion

The two component surfaces planned for investigation are shown in Figure 1. Two-component surfaces involving spacers **1**, **3**, **4**, and **6** have been prepared to date by the co-condensation of the phenolic spacer with HODPP in a single step as described above. The initial stoichiometries were adjusted to prepare surfaces at saturation coverage with similar spacer:DPP ratios (approximately 3:1).

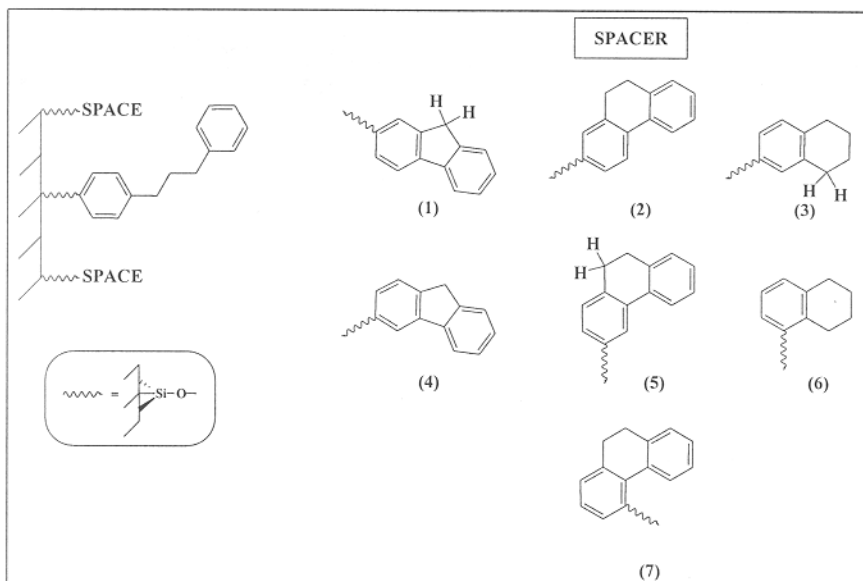


Figure 1. Silica-immobilized substrates to be studied.

Thermolyses were conducted at 375 °C in vacuum sealed Pyrex tubes. The major products (ca. 98 %) formed from the free-radical induced decomposition are shown below in Figure 2 along with the propagation steps from the radical chain mechanism (discussed below).

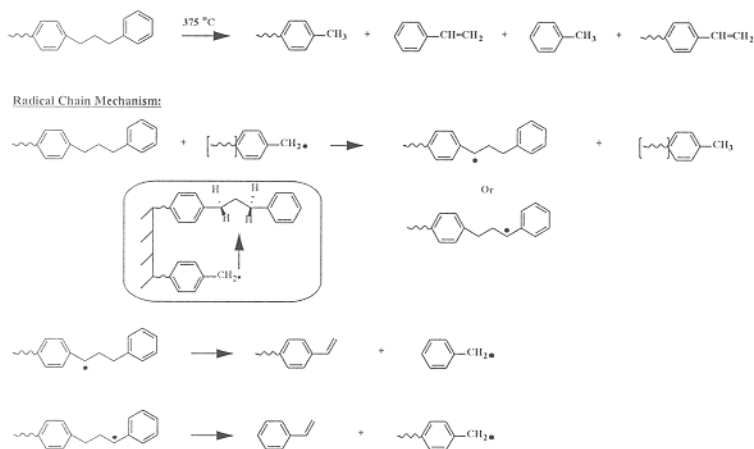


Figure 2. Major products formed from the radical induced decomposition of DPP.

Small amounts of surface-attached PhCH_2CH_3 (0.1-3.0 mol %) are also observed, as well as trace amounts of PhCH_2CH_3 (1.0 mol %). The only significant new product observed in the presence of the co-attached spacers occurs for the 2-fluorene case (3-11 mol % depending on DPP conversion) arising from addition of surface-attached fluorenyl radical to the surface-attached styrene.

Mass and stoichiometric balances are in good agreement indicating that all significant products are accounted for, see Table 1. The fragment balances are defined as $\text{C8}/\approx\text{C7}$ [$\text{PhCH}=\text{CH}_2/\approx\text{PhCH}_3$] and $\text{C7}/\approx\text{C8}$ [$\text{PhCH}_3/\approx\text{PhCH}=\text{CH}_2 + \approx\text{PhCH}_2\text{CH}_3$] and are close to the

value of unity required by stoichiometry (Table 1) with one exception. The C7/ \approx C8 balance in the 2-HOF1 spacer case is greater than 1 and increases with DPP conversion. This can be explained by the secondary reaction of surface attached *p*-vinyl phenol as described above. Selectivity is based on the ratio of gas phase styrene/toluene produced. The selectivity values reflect the relative rates for hydrogen abstraction by radicals (benzyl or spacer) from surface-attached DPP at the two benzylic positions, and are measured by the gas-phase styrene to toluene ratio (see Figure 2). At saturation surface coverages of DPP, or DPP with hydrogen donating spacers, selectivity values of ca. 0.92 (\pm 5 %) are generally obtained reflecting the stabilizing effect of the *p*-silyloxy substituent (surface linkage). The current examples are consistent with the previous findings with the exception of the 1-HOTET spacer. The value of 1.14 suggests that there is a geometric preference for abstracting the DPP benzylic hydrogen farthest from the surface. Additional insights may be obtained from molecular modeling studies.

Surface Component	Surface Coverage	Mass Balance	C8/ \approx C7	C7/ \approx C8	Selectivity	DPP Rate (%/h)
\approx DPP/ \approx 2-F1	0.156/0.426	101.9 \pm 1.6	0.94 \pm 0.07	1.55 \pm 0.2	0.89 \pm 0.03	67.5
\approx DPP/ \approx 3-F1	0.124/0.331	99.5 \pm 2.0	0.91 \pm 0.04	1.02 \pm 0.02	0.97 \pm .06	29.6
\approx DPP/ \approx 1-TET	0.0847/0.279	96.5 \pm 2.7	1.04 \pm 0.06	1.01 \pm 0.06	1.14 \pm 0.01	5.0
\approx DPP/ \approx 2-TET	0.11/0.45	100.4 \pm 3.7	0.99 \pm 0.1	0.91 \pm 0.12	0.92 \pm 0.01	15.1

Table 1. Impact of molecular orientation on thermolysis (375 °C) of DPP with isomeric spacer molecules.

The free radical chain mechanism for the decomposition of \approx DPP has been discussed elsewhere,^{1,3} but the key features are shown in Figure 2. Initiation by a small amount of C-C homolysis (74 kcal/mol) forms chain carrying benzyl radicals. The reaction is then propagated through hydrogen abstraction at the benzylic carbons of \approx DPP to form the gas-phase and surface-attached toluene products and radicals that can undergo β -scission to produce the surface attached and gas-phase styrene products. Termination occurs through coupling of the benzyl radical. The overall rate of decomposition of \approx DPP is governed by the rates of hydrogen transfer steps, which will be particularly sensitive to the surface coverage.

The initial reaction rates for \approx DPP at 375 °C in the presence of the spacer molecules were obtained from the slopes of linear regressions of \approx DPP conversion versus reaction times and the results are presented in Table 1. An example of the data is shown in Figure 3 for comparison of the two isomeric fluorene spacers. As expected, the \approx DPP decomposition rates increased with the addition of the hydrogen donor spacers relative to surfaces of \approx DPP at similar surface coverages without hydrogen donating spacers. However, it is clear that the rates are sensitive to the orientation of the spacer molecule on the surface. For example, the rate of DPP conversion

with the 2-FI spacer is 2.3x faster than that of 3-FI. Furthermore, the DPP conversion rate for the 2-TET spacer is 3x faster than 1-TET (see Figure 4 and Table 1).

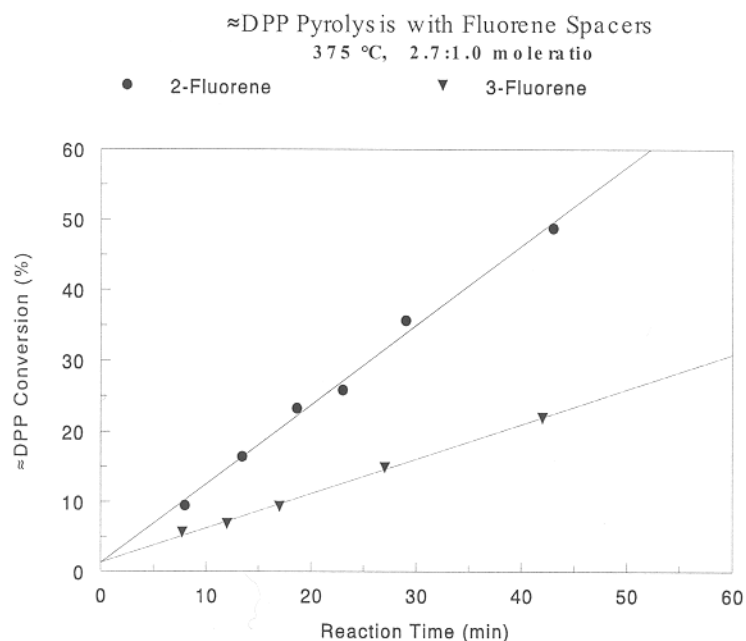


Figure 3. Rate plot of 2-HOFI and 3-HOFI.

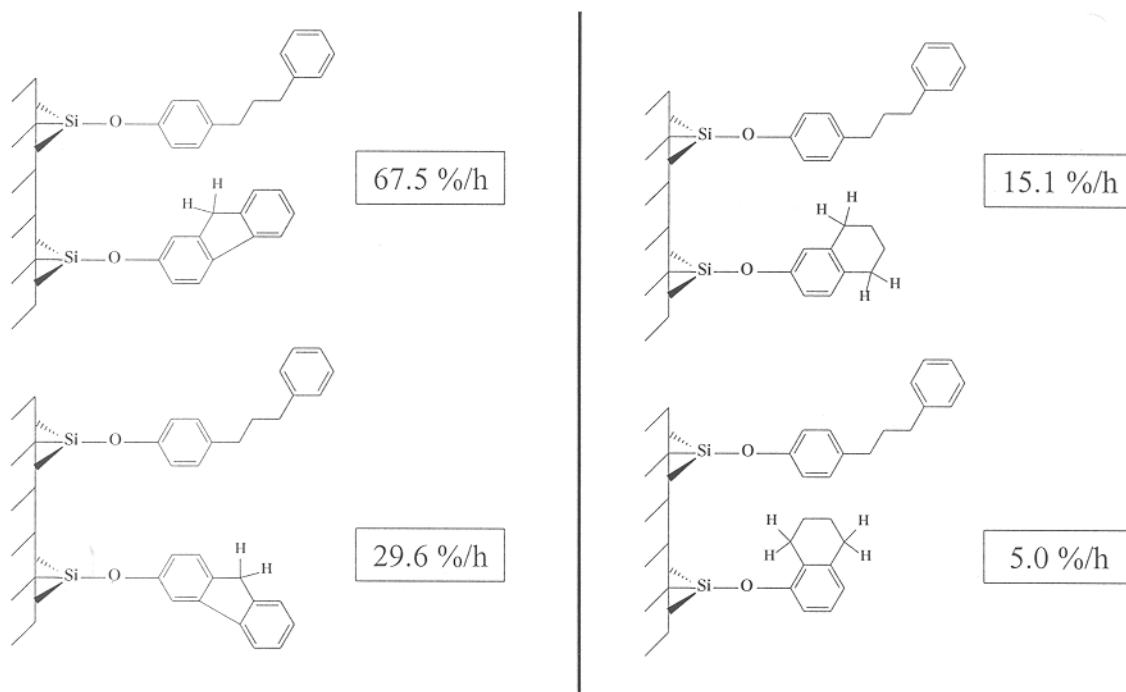


Figure 4. Influence of co-attached spacers, 2-FI, 3-FI, 2-TET, and 1-TET on the pyrolysis rate for DPP at 375°C.

The results suggest that a *meta*-orientation for the surface linkage, with respect to the donatable benzylic hydrogens, is the most efficient geometry for promoting the hydrogen transfer, radical relay process on the surface. This will be tested further with the two isomeric dihydrophenanthrene spacer molecules. Our prediction would be that the 2-DHP spacer will lead to a faster DPP pyrolysis rate than the 3-DHP isomer.

Conclusions

These pyrolysis studies clearly show that geometric constraints can play a large role in the rates of hydrogen transfer for free radical reactions under diffusional constraints. This provides new information on how the native structure of organic energy resources may control hydrogen utilization during thermal processing.

Acknowledgment.

This research was sponsored by the Division of Chemical Sciences, Geosciences, and Biosciences, Office of Basic Energy Sciences, U.S. Department of Energy under contract DE-AC05-00OR22725 with Oak Ridge National Laboratory, managed and operated by UT-Battelle, LLC. MKK was supported by an appointment to ORNL Postdoctoral Research Associated program administered jointly by Oak Ridge Institute for Science and Education and ORNL.

¹ (a) Buchanan, III, A. C.; Britt, P. F.; Thomas, K. B.; Biggs, C. A. *J. Am. Chem. Soc.* **1996**, *118*, 2182.

(b) Buchanan, III, A. C.; Britt, P. F.; Thomas, K. B.; Biggs, C. A. *Energy Fuels* **1993**, *7*, 373.

² (a) Buchanan, III, A. C.; Britt, P. F. *J. Anal. Appl. Pyrolysis* **2000**, *54*, 127. (b) Britt, P. F.; Buchanan, III, A. C.; Malcolm, E. A. *Energy Fuels* **2000**, *14*, 1314. (c) Buchanan, III, A. C.; Britt, P. F.; Skeen, J. T.; Struss, J. A.; Elam, C. L. *J. Org. Chem.* **1998**, *63*, 9895.

³ (a) Buchanan, A. C., III; Biggs, C. A. *J. Org. Chem.* **1989**, *54*, 517. (b) Poutsma, M. L.; Dyer, C. W. *J. Org. Chem.* **1982**, *47*, 4903. (c) Gilbert, K. E.; Gajewski, J. J. *J. Org. Chem.* **1982**, *47*, 4899. (d) Sweeting, J. W.; Wilshire, J. F. *Aust. J. Chem.* **1962**, *15*, 89. (e) King, H.-H.; Stock, L. M. *Fuel* **1982**, *61*, 1172.